

## ARTICLE

# Population-based cellular kinetic characterization of ciltacabtagene autoleucel in subjects with relapsed or refractory multiple myeloma

Liviawati S. Wu<sup>1</sup> | Yaming Su<sup>2</sup> | Claire Li<sup>3</sup> | Wangda Zhou<sup>3</sup> | Carolyn C. Jackson<sup>2</sup> | Yu-Nien Sun<sup>3</sup> | Honghui Zhou<sup>3</sup>

<sup>1</sup>Janssen Research & Development, Brisbane, California, USA

<sup>2</sup>Janssen Research and Development, Raritan, New Jersey, USA

<sup>3</sup>Janssen Research and Development, Spring House, Pennsylvania, USA

## Correspondence

Liviawati S. Wu, Janssen Research & Development, 1600 Sierra Point Parkway, Brisbane, CA 94005, USA.  
Email: [lwu79@its.jnj.com](mailto:lwu79@its.jnj.com)

## Present address

Yu-Nien Sun, Cognigen Division, Simulations Plus, Buffalo, New York, USA

Honghui Zhou, Elevar Therapeutics, Salt Lake City, Utah, USA

## Abstract

The aims of this work were to develop a population pharmacokinetic (PK) model for chimeric antigen receptor (CAR) transgene after single intravenous infusion administration of ciltacabtagene autoleucel in adult patients with relapsed or refractory multiple myeloma. CAR transgene level in blood were measured by quantitative polymerase chain reaction (qPCR) from 97 subjects in a phase Ib/II CARTITUDE-1 study (NCT03548207), with a targeted cilta-cel dose of  $0.75 \times 10^6$  (range  $0.5\text{--}1.0 \times 10^6$ ) CAR positive viable T-cells per kg body weight. The population PK model development was primarily guided by the current mechanistic understanding of CAR-T kinetics and the principles of building a parsimonious model. Cilta-cel PK was adequately described by a two-compartment model (with a fast and a slow apparent decline rate from each compartment, respectively) and a chain of four transit compartments with a lag time empirically representing the process from infused CAR-T cell to measurable CAR transgene. No apparent relationship was observed between cilta-cel dose (i.e., the actual number of CAR positive viable T-cells infused), given the narrow dose range, and the observed transgene level. Based on covariate search and subgroup analysis of maximum systemic CAR transgene level ( $C_{\max}$ ) and area under curve from the first dose to day 28 ( $AUC_{0-28d}$ ), none of the investigated subjects' demographics, baseline characteristics, and manufactured product characteristics had significant effects on cilta-cel PK. The developed model is deemed robust and adequate for enabling subsequent exposure-safety and exposure-efficacy analyses.

## Study Highlights

### WHAT IS THE CURRENT KNOWLEDGE ON THE TOPIC?

Ciltacabtagene autoleucel is a B-cell maturation antigen (BCMA)-directed CAR-T indicated for the treatment of relapsed/refractory multiple myeloma. CAR-T cellular kinetics time profiles often exhibit large intersubject variability.

This is an open access article under the terms of the [Creative Commons Attribution-NonCommercial-NoDerivs](https://creativecommons.org/licenses/by-nc-nd/4.0/) License, which permits use and distribution in any medium, provided the original work is properly cited, the use is non-commercial and no modifications or adaptations are made.

© 2022 Janssen Research & Development. *Clinical and Translational Science* published by Wiley Periodicals LLC on behalf of American Society for Clinical Pharmacology and Therapeutics.

Mathematical models using piecewise equations and analytical biexponential equation have been used for tisagenlecleucel and lisocabtagene maraleucel, however, the transgene kinetic profiles observed in the case of cilta-cel require a more flexible model structure.

#### **WHAT QUESTION DID THIS STUDY ADDRESS?**

The CAR-T cellular kinetic with transition function can adequately characterize CAR transgene level of cilta-cel in blood following i.v. infusion at the targeted cilta-cel dose of  $0.75 \times 10^6$  (range  $0.5\text{--}1.0 \times 10^6$ ) CAR-positive viable T-cells/kg body weight, based on data from the CARTITUDE-1 study.

#### **WHAT DOES THIS STUDY ADD TO OUR KNOWLEDGE?**

This is the first report describing the population cellular kinetic modeling of anti-BCMA CAR transgene levels of cilta-cel in blood. Given the large intersubject variability at various aspects of cilta-cel kinetics postinfusion, none of the investigated subjects' demographics and baseline characteristics and manufactured product characteristics showed statistically significant effect on CAR transgene levels.

#### **HOW MIGHT THIS CHANGE CLINICAL PHARMACOLOGY OR TRANSLATIONAL SCIENCE?**

This analysis demonstrated the methodology of modeling CAR-T cellular kinetic profiles that allows greater flexibility in fitting the large variability in individual profiles, such as lag during early phase, smoother peaks, mono- as well as bi-phasic decline after the time of maximum concentration. The alternative model structure presented here will enable improved characterization of the transgene kinetic profiles of other CAR-T therapeutic modalities in the future.

## **INTRODUCTION**

Ciltacabtagene autoleucel (cilta-cel, CARVYKTI, JNJ-68284528) is a B-cell maturation antigen (BCMA)-directed genetically modified autologous T-cell immunotherapy indicated for the treatment of adult patients with relapsed or refractory multiple myeloma. The chimeric antigen receptor (CAR) consists of two BCMA-targeting single domain antibodies designed to confer avidity, a CD3  $\zeta$  signaling domain and a 4-1BB costimulatory domain. BCMA is an attractive target for cell therapy for multiple myeloma because BCMA expression is restricted in normal tissue but is primarily on late-stage B-cells, plasma cells and malignant B-lineage cells.<sup>1-3</sup>

Understanding of the CAR-T cellular kinetics is based on earlier theoretic work by De Boer et al.<sup>4,5</sup> Specifically, the cellular kinetics after CAR-T cell administration include complex interplay among T-cell trafficking, migration from peripheral blood to the bone marrow and other secondary lymphoid tissues, and the immune activation and proliferation upon binding of antigen, programmed apoptosis of activated lymphocytes, and long-term persistence of memory cells. Whereas there is value in developing a systems pharmacology model of these granular processes,<sup>6</sup> a parsimonious population-based disposition model with essential

components of cellular kinetics is desirable to (1) adequately describe CAR-T cell kinetics; (2) to explore covariates effect on the CAR transgene pharmacokinetics (PKs), and (3) to support exposure-efficacy and safety relationships analyses. Therefore, empirical mathematical models have been employed to support regulatory submissions of CAR-T therapies.

Some examples of empirical population cellular kinetic models for the recently approved CAR-T therapies are tisagenlecleucel in relapsed or refractory B-cell acute lymphoblastic leukemia,<sup>7</sup> and lisocabtagene maraleucel (liso-cel) in relapsed or refractory large B-cell lymphoma,<sup>8</sup> both targeted to bind the CD19 antigen. In both reports, transgene level as assessed by quantitative polymerase chain reaction (qPCR) were used as basis, and both models are largely similar in that they involved empirical piecewise equations to describe the expansion phase up to time to maximum concentration ( $T_{\max}$ ) and the biphasic decline phase (using two decline rate constants [or half-lives], and an estimated fraction of maximum concentration [ $C_{\max}$ ] for the second phase). A lag phase was added to the initial cellular expansion phase in the liso-cel model. Much of these time-related parameters usually have numerical estimation challenges in characterizing its interindividual variability (IIV).<sup>8</sup> This is similar to the case where transit compartment models may be preferred over a standard compartmental PK model with  $T_{\text{lag}}$ .<sup>9</sup>

The aims of this work, therefore, were to develop an alternative population-based cellular kinetic model to characterize cilta-cel CAR transgene levels following intravenous infusion based on data from the study CARTITUDE-1, as well as explore the IIV and investigate covariates that might influence cilta-cel kinetics.

## METHODS

### Clinical study data

The study CARTITUDE-1 (NCT03548207) is a single-arm, open-label, multicenter phase Ib/II study to evaluate

$$\text{Transgene copy number per } \mu\text{g genomic DNA} = \text{Transgene copy number per } \mu\text{g sample DNA} \times \frac{1}{\text{hApoB copy per } \mu\text{g sample DNA}} \times \frac{280,700 \text{ copies of hApoB}}{\mu\text{g genomic DNA}}$$

the safety and efficacy of cilta-cel, which main cohort included a total of 97 subjects.<sup>10</sup> In this study, a targeted cilta-cel dose of  $0.75 \times 10^6$  (range  $0.5\text{--}1.0 \times 10^6$ ) CAR-positive viable T-cells/kg body weight was administered 5–7 days after a lymphodepleting conditioning regimen ( $300 \text{ mg/m}^2$  cyclophosphamide,  $30 \text{ mg/m}^2$  fludarabine daily for 3 days). This study was sponsored and designed by Janssen Pharmaceuticals, Inc. and Legend Biotech., and done in accordance with the Declaration of Helsinki and International Conference on Harmonization guidelines for Good Clinical Practice. All patients provided written informed consent. An independent ethics committee or institutional review board at each study center approved the study protocol.

### Sample analysis

The qPCR method to quantitate the levels of ciltacabtagene autoleucel (cilta-cel) in blood was derived from two

$$\text{LLOQ (unit copy number per } \mu\text{g genomic DNA)} = \text{LLOQ (i. e., 50 copies per } \mu\text{g sample DNA)} \times \frac{1}{\text{hApoB copy per } \mu\text{g sample DNA}} \times \frac{280,700 \text{ copies of hApoB}}{\mu\text{g genomic DNA}}$$

separate qPCR assays. One assay specifically measured copies of the CAR transgene present in a sample. The second assay quantitated an endogenous human reference gene, ApoB. All study samples were analyzed using both methods.

Both assays were validated separately. The CAR transgene assay was validated with samples containing the

CAR transgene and 400 ng of genomic DNA per qPCR reaction. The lower limit of quantification (LLOQ) of this assay was 20 copies of CAR transgene per reaction or 50 copies/ $\mu\text{g}$  of sample DNA. The ApoB assay was performed with 100 ng of genomic DNA as template per qPCR reaction. The LLOQ for the ApoB assay is 20 copies per reaction or 200 copies/ $\mu\text{g}$  of sample DNA.

The results of both assays were combined, and the final result was calculated by normalizing the experimentally measured CAR copy number with the experimentally measured ApoB gene copy number in the same blood sample. The CAR-T copy number per  $\mu\text{g}$  of genomic DNA is determined using the theoretical number of hApoB copies from 1  $\mu\text{g}$  of human gDNA as detailed below:

The theoretical number of a unique DNA sequence like human ApoB per 1  $\mu\text{g}$  of human gDNA is calculated at 280,700 based on the following formula:

$$\frac{\left( \text{DNA in } \mu\text{g} \times \frac{10^{-6} \text{ g}}{\mu\text{g}} \times \frac{6.022 \times 10^{23} \text{ molecules}}{\text{mole}} \right)}{3.3 \times 10^9 \text{ bp} \times 650 \frac{\text{g}}{\text{bp}} / \text{mole}}$$

This calculation was based on the length of human haploid DNA at  $3.3 \times 10^9$  bp, the assumption that the average weight of 1 bp is 650 Daltons and Avogadro's number of  $6.022 \times 10^{23}$  molecules/mole.

This derived result was reported as CAR transgene with unit of “copies/ $\mu\text{g}$  genomic DNA” and used in the PK analysis. A single LLOQ value was not applicable for this final normalized result (i.e., the LLOQ of the CAR transgene assay [50 copies/ $\mu\text{g}$  of sample DNA] should not be regarded as the LLOQ of the ApoB normalized CAR transgene level [unit of copies/ $\mu\text{g}$  genomic DNA] intended for the PK analysis). Rather, the LLOQ was dependent on the ApoB copy number in the corresponding sample DNA, calculated as follows:

### Population modeling

The data were analyzed by a nonlinear mixed effects modeling approach implemented in NONMEM version 7.4.3.<sup>11</sup> The interindividual random effects on the parameters were modeled using MU referencing to add efficiency when using the stochastic approximation expectation maximization (SAEM) method. The standard error of parameter

estimates was obtained by importance sampling method. The residual error structure was assumed to follow a log-normal distribution (i.e., an additive normal distribution on the natural logarithm of the observations).

Any observation records before the start of infusion were excluded from the analysis. End-of-infusion samples that were quantifiable (i.e., above the LLOQ; 17 out of 97 subjects) were excluded because these samples were followed by the series of data below the limit of quantification (BLOQ), indicating a rapid margination phase. Any BLOQ preceding the last BLOQ before a quantifiable sample in the early phase prior to  $C_{max}$  and any BLOQ after the first BLOQ in the terminal phase were excluded. Sensitivity analysis was performed to confirm that these early and terminal subsequent BLOQ were not informative for building the current cellular kinetic model. The remaining BLOQ data were accounted for by using the M3 method.<sup>12-14</sup>

## Structural model

Stein et al.<sup>7</sup> used piecewise methods of exponential growth function prior to the  $T_{max}$  followed by biphasic decline after  $T_{max}$ . This model had six parameters:  $C_{max}$ , fraction that declined slowly ( $F_B$ ), rapid decline rate ( $\alpha$ ), gradual decline rate ( $\beta$ ), fold expansion from baseline ( $fold_x$ ), and  $T_{max}$ . However, because a large portion of the early time-points in cilta-cel CAR transgene data were BLOQ, the estimation of  $fold_x$  parameter could not be achieved in the current data.

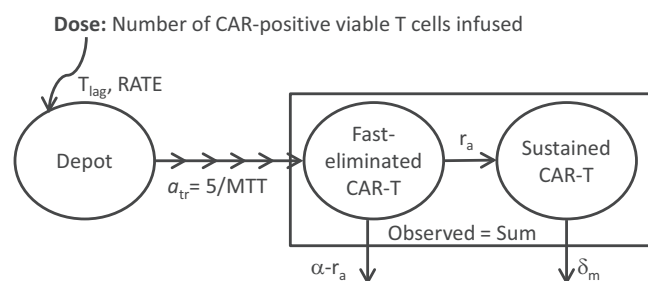


**FIGURE 1** Ciltacabtagene autoleucel CAR transgene kinetic model diagram. CAR-T = chimeric antigen receptor T cell;  $T_{lag}$  = apparent lag time for margination and appearance; MTT = apparent mean transit time;  $\alpha$  = apparent rapid decline rate;  $r_a$  = apparent transition rate from fast eliminated to sustained CAR-T;  $\delta_m$  = apparent gradual decline rate. Dose of CAR-positive viable T-cells (target dose  $0.75 \times 10^6$  cells/kg) was infused into the depot compartment. A series of four transit compartments was used to characterize the initial appearance and proliferation of CAR T cells. The CAR transgene level observation was defined as the sum of the fast-eliminated CAR-T and sustained CAR T compartments.

Hence, another model structure was proposed (Figure 1), where typical PK absorption models such as lag time and a series of transit compartments<sup>9</sup> were applied to describe the initial CAR-T redistribution and expansion, and two compartments with fast and slow decline rate from each compartment, respectively. The proposed model had five parameters with notation similar to the De Boer model<sup>4</sup>: apparent rapid decline rate ( $\alpha$ ), apparent transition rate to longer-lived CAR T ( $r_a$ ), apparent gradual decline rate ( $\delta_m$ ), apparent mean transit time (MTT), and apparent lag time for margination and appearance ( $T_{lag}$ ). These parameters empirically describe the conversion from the dose of viable CAR-positive T cells to CAR transgene level, which involves aggregate physiological processes such as initial margination, expansion, differentiation, contraction, and persistence.

## Covariate analyses

The following steps briefly describe the covariate analysis for the cilta-cel PK model.

Step 1, graphical exploration was performed to investigate the influence on PK parameters of a list of potential covariates: age, sex, race, body weight, baseline serum soluble BCMA, serum albumin baseline level, creatinine clearance, hepatic function, type of myeloma, Eastern Cooperative Oncology Group (ECOG) score, staging (International Staging System [ISS]), cytogenetic risk, baseline serum M-protein, kappa and lambda free light chain, bone marrow percent plasma cells, tumor BCMA expression, tumor burden, baseline hemoglobin, platelets, lymphocytes, leukocytes, neutrophils, number of prior lines of therapy, prior autologous transplantation, prior allogeneic transplantation, bridging therapy administration, and the manufactured product characteristics (percent CD4+ cells, percent CD8+ cells, CD4/CD8 ratio, transduction efficiency, CAR expression, percent CAR+ naive, percent CAR+ effector, percent CAR+ central memory, percent CAR+ effector memory, percent CAR- naive, percent CAR- effector, percent CAR- central memory, percent CAR- effector memory, percent CD3+ cells, CD3+ viability, in vitro tumor kill assay, vector copy number, viable nucleated cells, post thaw viability; a baseline value was defined as closest non-missing value before the initial dose of cilta-cel, with the exception of parameters associated with disease-related efficacy assessment, for which the baseline value is defined as the non-missing value closest to the start of conditioning regimen and before cilta-cel infusion). This led to a subset of covariates for statistical significance testing.

Step 2, all parameter-covariate relationships that have a significant correlation ( $p < 0.01$ ; e.g., sex, body weight,

and baseline serum soluble BCMA) were included into a population PK model as the full model.

Step 3, starting from the full model, backward elimination was applied following likelihood ratio test, where parameter-covariate relationships were removed from the model if they did not result in a statistically significant ( $p < 0.001$ ) increase of the objective function value. The resulting model was considered as the final model.

Covariate relationships were included multiplicatively as power models (continuous covariates) or as conditional effects relative to the most common category (categorical covariates).

For continuous covariates:

$$P_j = \theta_0 \cdot \left( \frac{X_{ij}}{M(X_j)} \right)^{\theta_j}$$

For discrete covariates:

$$P_j = \theta_0 \cdot \theta_j^{X_{ij}}$$

where  $P_j$  is the  $j$ -th population estimate of parameters,  $X_{ij}$  is the covariate of subject  $i$  for the parameter  $P_j$ ,  $M(X_j)$  is the median of covariate  $X$  for the population,  $\theta_0$  is the typical value of the parameter  $P_j$ , and  $\theta_j$  is a constant that reflect the covariate's effect on the parameter.

## Model evaluation

Model evaluation/qualification assessed various goodness-of-fit measures, including parameter estimates relative standard error (RSE), standard diagnostic plots, and visual predictive check (VPC) based on 1000 replicates. Bootstrap median and 95% confidence interval (CI) values were also obtained based on 500 bootstrap datasets.<sup>15</sup> The final model was deemed adequate if it was consistent with the existing knowledge of CAR-T PK and provided a good description of the observed data with no apparent bias in the relevant goodness-of-fit diagnostics.

## Simulations

The final population-based cellular kinetic model was subsequently used to simulate the individual predicted exposure metrics:  $C_{\max}$ , maximum transgene levels and area under the curve (AUC) for transgene levels from 0 to day 28 ( $AUC_{0-28d}$ ). Subgroup analyses were used to further explore the impact of covariates on cilta-cel exposure.

## RESULTS

The population analysis dataset included 1306 cilta-cel transgene levels from all 97 subjects in the CARTITUDE-1 study. Following a single intravenous infusion, cilta-cel exhibited an initial expansion phase followed by a rapid decline and then a slower decline with persistence over months. High IIV was observed.

Table 1 summarizes the dose, demographic, and baseline characteristics of the patients. Median age was 62 years (range: 43–78 years). The median of the last PK timepoints was 11.7 months (range: 1.2–23.4 months).

The population-based cellular kinetic model parameter estimates are presented in Table 2, including bootstrap median and 95% CI for each parameter ( $n = 500$  bootstrap datasets). The proportional residual error accounting for intra-individual and other unexplained variability in cilta-cel CAR transgene data was estimated to be 0.826. No apparent systematic deviations or trends were noticed in any of the goodness-of-fit plots, including VPC, residual plots, and the empirical Bayes estimates (EBEs) of ETAs versus covariates plots. All parameters were estimated reasonably well with %RSE <15% and IIV shrinkage<sup>16</sup> <30%.

The bootstrap runs were run with SAEM method. All 500 runs successfully reached stationarity during the burn-in phase (NBURN = 2000) and completed the NITER = 1000 iterations. The bootstrap median and 95% CI values are in close agreement with the original parameter estimates, indicating acceptable robustness of the model (Figure S1). A sample of individual fits are included in Figure S2.

Figure 2 shows the VPC of the final model overlaying the observed and model-predicted cilta-cel transgene level versus time postdose. The median, 10th, and 90th percentiles of the observed data were in agreement with the 95% CI of the median, 10th, and 90th percentiles of the simulated data, respectively. The model reasonably characterized the timing and peak CAR transgene level and the possible mono- or bi-exponential decline in the individual CAR transgene time profiles (Figure S2). Summaries of descriptive statistics of the individual model parameter estimates are presented in Table 3.

The model-predicted geometric mean of the individual  $C_{\max}$  and  $AUC_{0-28d}$  were compared across different strata for each covariate in Figure 3a and b, respectively. None of the 95% CIs for the estimated geometric mean ratio of cilta-cel CAR transgene  $C_{\max}$  and  $AUC_{0-28d}$  across strata of specific covariates included the null value (i.e., geometric mean ratio of 1). Although sex was found to be a statistically significant covariate on the  $\alpha$  parameter ( $p$  value <0.001, associated with change in minimum objective function value [MOFV] >10.83) in the cilta-cel kinetic

**TABLE 1** Summary of dose, demographics, baseline covariates, and other characteristics

Phase	Phase Ib	Phase II	Total
<i>N</i>	29	68	97
Total CAR+ viable T-cells (10 <sup>6</sup> cells)			
Mean (SD)	59.8 (13.4)	54.7 (13.7)	56.2 (13.7)
Median	59.0	51.5	54.3
Range	35.7–82.0	23.5–93.1	23.5–93.1
Total CAR+ viable T-cells/kg (10 <sup>6</sup> cells/kg)			
Mean (SD)	0.710 (0.0877)	0.710 (0.0904)	0.710 (0.0892)
Median	0.722	0.707	0.709
Range	0.519–0.894	0.509–0.954	0.509–0.954
Weight, kg			
Mean (SD)	84.6 (16.7)	76.9 (16.3)	79.2 (16.7)
Median	83.1	76.6	78.3
Range	54.5–121	39–126	39–126
Age, years			
Mean (SD)	60.9 (6.42)	62.5 (9.09)	62.0 (8.38)
Median	60	62	61
Range	50–75	43–78	43–78
Sex, <i>n</i>			
Male	14 (48.3%)	43 (63.2%)	57 (58.8%)
Female	15 (51.7%)	25 (36.8%)	40 (41.2%)
Race, <i>n</i>			
White	20 (69.0%)	49 (72.1%)	69 (71.1%)
Black, of African heritage or African American	5 (17.2%)	12 (17.6%)	17 (17.5%)
Other	4 (13.8%)	7 (10.3%)	11 (11.3%)
Ethnicity, <i>n</i>			
Not Hispanic or Latino	25 (86.2%)	60 (88.2%)	85 (87.6%)
Hispanic or Latino	2 (6.9%)	4 (5.9%)	6 (6.2%)
Not reported	2 (6.9%)	4 (5.9%)	6 (6.2%)
Renal function, ml/min, <i>n</i>			
CRCL ≥90	24 (82.8%)	33 (48.5%)	57 (58.8%)
60 ≤ CRCL <90	4 (13.8%)	26 (38.2%)	30 (30.9%)
30 ≤ CRCL <60	1 (3.4%)	9 (13.2%)	10 (10.3%)
Hepatic function, <i>n</i>			
Normal	25 (86.2%)	60 (88.2%)	85 (87.6%)
Mild dysfunction	4 (13.8%)	8 (11.8%)	12 (12.4%)
Baseline hemoglobin, g/L			
Mean (SD)	93.9 (15.6)	93.4 (14.1)	93.6 (14.5)
Median	96.0	89.0	90.0
Range	68–129	69–129	68–129
Baseline platelets, 10 <sup>9</sup> /L			
Mean (SD)	155 (81.9)	143 (78.3)	146 (79.2)
Median	161	134	138
Range	12–347	24–427	12–427

(Continues)

TABLE 1 (Continued)

Phase	Phase Ib	Phase II	Total
Baseline lymphocytes, 10 <sup>9</sup> /L			
Mean (SD)	0.0938 (0.295)	0.0694 (0.171)	0.0767 (0.214)
Median	0.02	0.03	0.03
Range	0.00–1.60	0.00–1.40	0.00–1.60
Baseline leukocytes, 10 <sup>9</sup> /L			
Mean (SD)	1.37 (0.677)	1.35 (0.812)	1.36 (0.771)
Median	1.40	1.20	1.20
Range	0.30–3.20	0.12–3.70	0.12–3.70
Baseline neutrophils, 10 <sup>9</sup> /L			
Mean (SD)	1.20 (0.641)	1.19 (0.735)	1.19 (0.705)
Median	1.17	1.00	1.10
Range	0.30–3.00	0.11–3.60	0.11–3.60
Type of myeloma, <i>n</i>			
IgG	16 (55.2%)	41 (60.3%)	57 (58.8%)
Non-IgG	13 (44.8%)	27 (39.7%)	40 (41.2%)
Baseline cytogenetic risk, <i>n</i>			
Standard risk	22 (75.9%)	46 (67.6%)	68 (70.1%)
High risk	7 (24.1%)	16 (23.5%)	23 (23.7%)
Unknown	0 (0%)	6 (8.8%)	6 (6.2%)
ECOG status, <i>n</i>			
0	12 (41.4%)	27 (39.7%)	39 (40.2%)
1	14 (48.3%)	40 (58.8%)	54 (55.7%)
2	3 (10.3%)	1 (1.5%)	4 (4.1%)
Baseline ISS staging, <i>n</i>			
I	20 (69.0%)	41 (60.3%)	61 (62.9%)
II	9 (31.0%)	13 (19.1%)	22 (22.7%)
II	0 (0.0%)	14 (20.6%)	14 (14.4%)
Time since MM diagnosis, years			
Mean (SD)	6.16 (3.53)	7.11 (3.64)	6.82 (3.62)
Median	5.05	6.65	5.94
Range	1.58–16.3	1.61–18.2	1.58–18.2
Baseline serum BCMA, ng/ml			
Mean (SD)	78.3 (100)	191 (268)	157 (235)
Median	37.1	74.1	58.5
Range	4.94–476	3.70–1340	3.70–1340
Unknown, <i>n</i>	0 (0%)	1 (1.5%)	1 (1.0%)
Baseline bone marrow % plasma cells			
≤30	17 (58.6%)	41 (60.3%)	58 (59.8%)
>30–<60	5 (17.2%)	12 (17.6%)	17 (17.5%)
≥60	7 (24.1%)	14 (20.6%)	21 (21.6%)
Unknown, <i>n</i>	0 (0.0%)	1 (1.5%)	1 (1.0%)
Baseline tumor BCMA expression, <i>n</i>			
<Median value	9 (31.0%)	26 (38.2%)	35 (36.1%)
≥Median value	8 (27.6%)	23 (33.8%)	31 (32.0%)

**TABLE 1** (Continued)

Phase	Phase Ib	Phase II	Total
Unknown	12 (41.4%)	19 (27.9%)	31 (32.0%)
Baseline tumor burden category, <sup>a</sup> <i>n</i>			
Low	16 (55.2%)	43 (63.2%)	59 (60.8%)
Intermediate	10 (34.5%)	12 (17.6%)	22 (22.7%)
High	3 (10.3%)	13 (19.1%)	16 (16.5%)
Number of lines of prior therapy, <i>n</i>			
≤4 lines	10 (34.5%)	23 (33.8%)	33 (34.0%)
>4 lines	19 (65.5%)	45 (66.2%)	64 (66.0%)
Prior autologous stem cell transplant, <i>n</i>			
No	3 (10.3%)	7 (10.3%)	10 (10.3%)
Yes	26 (89.7%)	61 (89.7%)	87 (89.7%)
Prior allogenic stem cell transplant, <i>n</i>			
No	29 (100.0%)	60 (88.2%)	89 (91.8%)
Yes	0 (0.0%)	8 (11.8%)	8 (8.2%)
Bridging therapy, <sup>b</sup> <i>n</i>			
No	6 (20.7%)	18 (26.5%)	24 (24.7%)
Yes	23 (79.3%)	50 (73.5%)	73 (75.3%)

Abbreviations: BCMA, B-cell maturation antigen; CAR, chimeric antigen receptor; CRCL, creatinine clearance by Cockcroft-Gault formula; ECOG, Eastern Cooperative Oncology Group; Ig, immunoglobulin; ISS, International Staging System; MM, multiple myeloma; *n*, number of subjects; SD, standard deviation.

<sup>a</sup>Tumor burden category definition: High: Any of the following parameters at baseline were met: Bone marrow % plasma cell ≥80%; Serum M-spike ≥5 g/dl; Serum free light chain ≥5000 mg/L. Low: All of the following (as applicable to the subject) parameters at baseline were met: Bone marrow % plasma cell <50%; Serum M-spike <3 g/dl; Serum free light chain <3000 mg/L. Intermediate: Did not fit either criteria of high or low tumor burden.

<sup>b</sup>Bridging therapy was administered between the time of apheresis and the first dose of the conditioning regimen.

**TABLE 2** Model parameter estimates

Parameters <sup>a</sup>	Description	Estimate <sup>a</sup> (%RSE)	exp (Est) <sup>b</sup>	IIV variance	IIV %CV <sup>c</sup> (%RSE) <sup>d</sup>	Shrinkage <sup>e</sup> (%)
$T_{lag}$ , days	Lag time for margination and appearance	1.56 (1.82)	4.76	0.0454	21.6 (12.8)	14.5
MTT, days	Mean transit time (to reparameterize $a_{tr}$ )	2.36 (1.65)	10.6	0.0573	24.3 (13.0)	29.1
$\alpha$ , day <sup>-1</sup>	Rapid decline rate	5.20 (1.94)	181	0.52	82.6 (10.8)	21.4
$r_a$ , day <sup>-1</sup>	Rate constant for apparent transition	-4.55 (6.46)	0.0106	4.27	840 (11.4)	17.8
$\delta_m$ , day <sup>-1</sup>	Gradual decline rate	-3.85 (4.57)	0.0213	2.09	266 (14.2)	12.7
Proportional residual error $\theta$ term <sup>f</sup>		0.826 (2.63)	-	-	-	-

Abbreviations:  $a_{tr}$ , rate constant for transition to the next transit compartment, defined as 5/MTT;  $C_{obs}$ , observed concentration;  $C_{pred}$ , predicted concentration; CV, coefficient of variation; exp(Est), model parameter estimates; IIV, interindividual variability; RSE, relative standard error.

<sup>a</sup>Model parameters were estimated in natural log domain.

<sup>b</sup>Model parameters were converted to the normal scale.

<sup>c</sup>IIV %CV = 100 × square root(exp[IIV variance]-1).

<sup>d</sup>RSE for IIV = (SE/variance estimate)/2.

<sup>e</sup>Shrinkage = 1-SD (IIVposthoc)/square-root (IIV variance).

<sup>f</sup>Residual error was parameterized for the log-transformed data as  $\ln(C_{obs}) = \ln(C_{pred}) + \theta \cdot \text{EPS}(1)$ , where  $\theta$  is the standard deviation and EPS(1) is a normally distributed error with mean 0 and variance fixed to 1.

model during covariate search by backward elimination, a physiologically plausible explanation for this effect is not readily available. In addition, the 95% CI for the geometric mean ratio of  $C_{max}$  and  $AUC_{0-28d}$  of female versus male

subjects included the null value (i.e., geometric mean ratio of 1). Therefore, the base model (i.e., the model without any covariates) was still determined as the final model from a parsimonious perspective.



## DISCUSSION

The observed cilta-cel CAR transgene kinetic data were adequately described by a two-compartment model and a chain of four transit compartments with lag time empirically representing the process from infused CAR-T to measurable CAR transgene. IIV were estimated on all five parameters:  $T_{lag}$ , MTT,  $\alpha$ ,  $r_a$ , and  $\delta_m$ . These parameters empirically describe the conversion from the dose of viable CAR-positive T cells to CAR transgene level, which involves aggregate physiological processes such

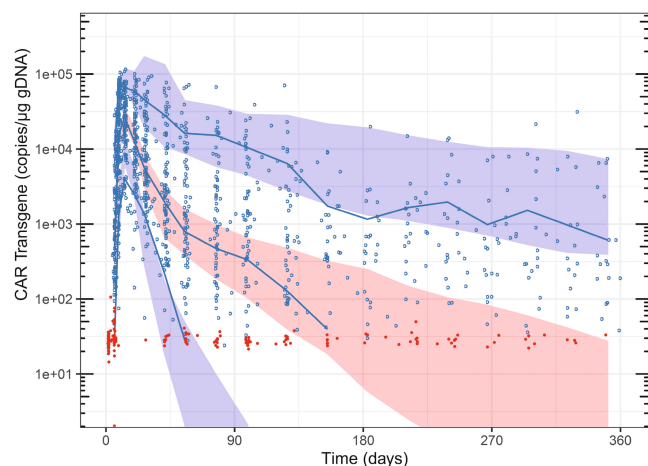


**FIGURE 2** Visual predictive check final population cellular kinetic model. Blue circles are observed CAR transgene observations. Solid lines are median, 10th and 90th percentiles of the observed data. Pink shaded area represents the 95% CI of the median and purple shaded areas represent the 95% CI of the 10th and 90th percentiles of the simulation (1000 replicates). Red points are BLOQ data where the LLOQ was derived as  $(280,700 \times 50) / \text{hApob copy number per } \mu\text{g sample DNA}$ . BLOQ, below the limit of quantification; CAR, chimeric antigen receptor; CI, confidence interval; gDNA, genomic DNA; LLOQ, lower limit of quantification

as initial T-cell margination, expansion, differentiation, contraction, and persistence.

The two compartments were designated as fast-eliminated and sustained CAR-T to convey that the model is indeed empirical and not representing distinct phenotype of T-cells, whether effector or memory CAR-T cells. There is also no mass balance and no volume of distribution-like scaling parameter as in a typical compartmental PK model due to the inconsistent units between the amount (CAR-positive viable T cells) and transgene level (copies per  $\mu\text{g}$  genomic DNA).

The population cellular kinetic model described above adequately captured the central tendency and variability in observations from patients in the CARTITUDE-1 study and parameter estimates agree well with the bootstrap values, indicating parsimony and stability of the model, with no systemic biases in the model fit.

The introduction of transit compartments to describe oral absorption delay in Savic et al. yielded an estimate of MTT around 0.5 h,<sup>9</sup> to substitute for lag time which was estimated as around 0.3 h. Comparatively, the current model used both the lag time and the transit compartments and estimated  $T_{lag}$  of 4.76 days and MTT of 10.6 days, which along with the corresponding IIV, yielded individual predicted  $T_{max}$  ranging from 10 to 25 days (Table 3). Although the original application in Savic et al. was to describe a delay in the order of <1 h, the construct of transit compartments is actually versatile in describing a much longer delay (e.g., in the order of <1 month for CAR-T kinetics).

The current model selected four transit compartments after comparing alternative models with two, three, and five transit compartments. The choice of model was based on comparison of MOFV, IIV, residual variability, and parameters RSEs. The model with two transit compartments had high IIVs even though residual variability was

**TABLE 3** Summary statistics of individual model parameters and model-predicted exposure metrics

	Mean	SD	Min	5th %	Median	95th %	Max
$T_{lag}$ , days	4.99	0.869	3.31	3.88	4.85	6.79	8.22
MTT, days	10.4	1.76	6.16	8.10	10.1	13.5	15.7
$\alpha$ , $\text{day}^{-1}$	209	148	66.7	83.2	160	561	739
$r_a$ , $\text{day}^{-1}$	0.0410	0.0644	0.0000778	0.00114	0.0154	0.183	0.387
$\delta_m$ , $\text{day}^{-1}$	0.0525	0.0617	0.000538	0.00519	0.0238	0.192	0.279
$C_{max}$ , copies/ $\mu\text{g}$ genomic DNA	39,520	23,300	5560	11,800	34,200	83,200	123,000
$AUC_{0-28d}$ , day·copies/ $\mu\text{g}$ genomic DNA	472,000	325,000	69,300	116,000	371,000	1,150,000	1,550,000
$T_{max}$ , days	14.1	2.41	10	11	14	17.2	25
$T_{BLOQ}$ , days	345	675	26.8	37.4	170	1110	6300

Abbreviations:  $AUC_{0-28d}$ , area under the CAR transgene systemic level-time curve from the first dose to Day 28 in units of day·copies/ $\mu\text{g}$  genomic DNA (model-predicted);  $C_{max}$ , maximum CAR transgene systemic level in units of copies/ $\mu\text{g}$  genomic DNA (model-predicted); MTT, mean transit time;  $r_a$ , transition rate to longer-lived CAR-T; SD, standard deviation;  $T_{BLOQ}$ , time of CAR transgene systemic level reaching 50 copies/ $\mu\text{g}$  genomic DNA (model-predicted);  $T_{lag}$ , lag time for margination and appearance;  $T_{max}$ , time of maximum CAR transgene systemic level in days (model-predicted);  $\alpha$ , rapid decline rate;  $\delta_m$ , gradual decline rate.

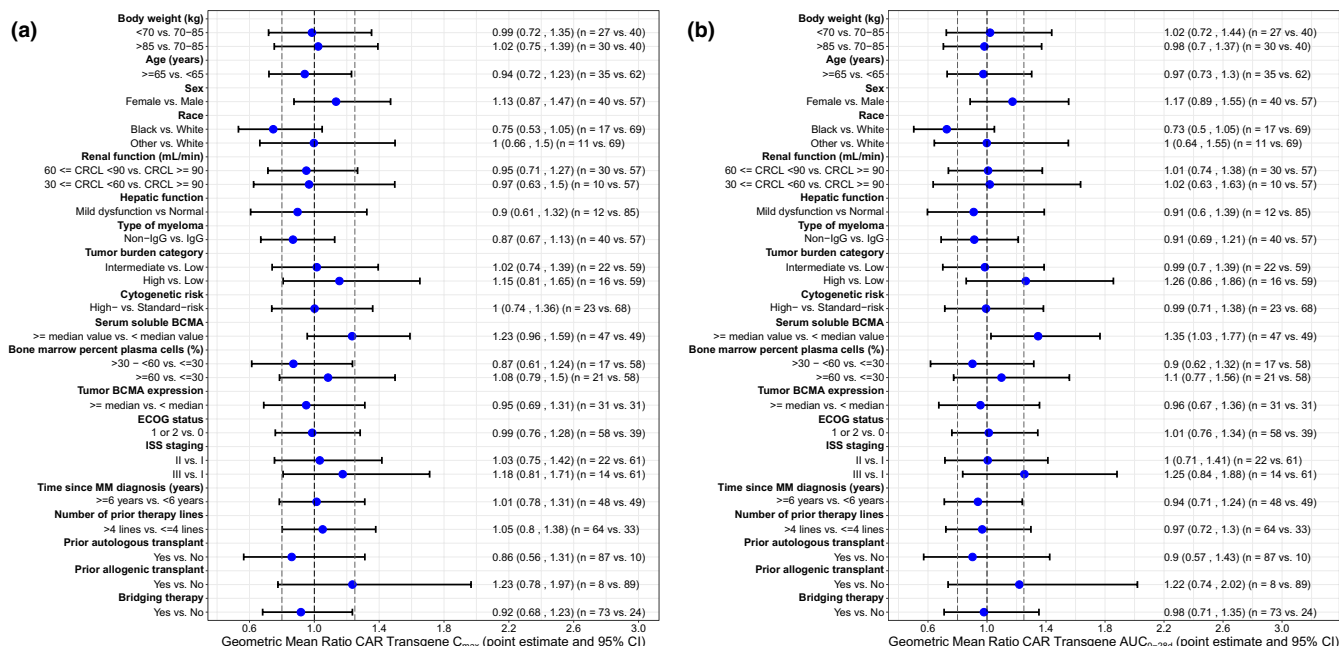


**FIGURE 3** (a) Forest plot of CAR transgene C<sub>max</sub>. (b) Forest plot of CAR transgene AUC<sub>0-28d</sub>. Data were log-transformed to calculate the geometric mean ratio (blue points) and the corresponding 95% CI (black horizontal segments). The associated values are shown on the right column. The dashed vertical lines refer to 0.8 and 1.25, respectively. Tumor burden category definition (High/Low/Intermediate): High, any of the following parameters at baseline were met: bone marrow percentage plasma cell ≥80%; serum M-spike ≥5 g/dl; serum free light chain ≥5000 mg/L. Low, all of the following (as applicable to the subject) parameters at baseline were met: bone marrow percentage plasma cell <50%; serum M-spike <3 g/dl; serum free light chain <3000 mg/L. Intermediate, did not fit either criteria of high or low tumor burden. Bridging therapy was administered between the time of apheresis and the first dose of the conditioning regimen. AUC<sub>0-28d</sub>, area under the CAR transgene systemic level-time curve from the first dose to day 28 (model-predicted); BCMA, B-cell maturation antigen; CAR, chimeric antigen receptor; CI, confidence interval; C<sub>max</sub>, maximum CAR transgene systemic level (model-predicted); CRCL, creatinine clearance; ECOG, Eastern Cooperative Oncology Group; Ig, immunoglobulin; ISS, International Staging System; MM, multiple myeloma; PPK, population pharmacokinetics

the lowest. The model with three transit compartments had the lowest MOFV (1791), lowest residual variability (0.820), lower IIV  $T_{lag}$  (18.7 vs. 21.6 percent coefficient of variation [%CV]), but the other four IIVs were higher compared to the final model with four transit compartments (26.7 vs. 24.3, 85.8 vs. 82.6, 1070 vs. 840, and 268 vs. 266 %CV for MTT,  $\alpha$ ,  $r_a$ , and  $\delta_m$ , respectively). The final model with four transit compartments also had lower MOFV (1815 vs. 1844), lower residual variability (0.826 vs. 0.840), lower RSE on majority of the parameters, and lower IIV  $T_{lag}$  (21.6 vs. 24.7 %CV) than the model with five transit compartments, whereas the other four IIVs were higher (24.3 vs. 23.5, 82.6 vs. 81.4, 840 vs. 732, and 266 vs. 250 %CV for MTT,  $\alpha$ ,  $r_a$ , and  $\delta_m$ , respectively). Therefore, the model with four compartments were chosen as the final model structure, acknowledging the trade-off of the factors described above.

Compared to the initial De Boer model for T-cell response to lymphocytic choriomeningitis virus (LCMV),<sup>4</sup> which included the parameters related to recruitment times ( $T_{on}$  and  $T_{off}$ ) and proliferation rate ( $\rho$ ) to describe the phase prior to the peak, the current model uses the

CAR-T infused cells amount entering the model system with lag time and transit compartments delay parameters ( $T_{lag}$  and MTT) to produce the similar trajectory without having to constraint an on-and-off switch that may pose numerical instability. The De Boer model also had challenges in fitting all the parameters at once, which led the authors to assume the rate constant for memory cell death,  $\delta_m$ , fixed to  $10^{-5} \text{ day}^{-1}$ , and the rate constant for memory cell reactivation,  $\alpha$ , to  $1 \text{ day}^{-1}$ . Accordingly, to follow model parsimony principles, the current model did not include the reactivation from the sustained CAR-T back to the fast-eliminated CAR-T, but rather only estimated the net apparent transition from fast-eliminated CAR-T to sustained CAR-T using the rate constant  $r_a$ . Although the estimate of  $r_a$  were similar at  $0.01 \text{ day}^{-1}$ , there are some caveats in directly comparing the parameter values between these two models because the models had different settings (CAR-T transgene in patients who underwent lymphodepletion vs. T cell response to LCMV).

Compared to the previous models of CAR-T transgene,<sup>7,8</sup> the current model allows inclusion of the number

of CAR-positive viable T cells infused (range in this dataset:  $23.5\text{--}93.1 \times 10^6$  CAR-positive viable T-cells), estimation of IIV for all five parameters, flexibility of fitting smoother peaks, incorporating BLOQ data using M3 method, and fitting of mono- as well as biphasic decline after the  $T_{\max}$ . In addition to the increased flexibility, the current model structure also overcomes the challenges of high shrinkage in estimating IIV on the time-related parameters, as mentioned in previous model.<sup>7,8</sup> For example, IIV for  $\text{fold}_x$ ,  $F_B$ , and  $\beta$  in the Stein model were higher than 30%, and similarly, IIV for  $T_{\text{gro}}$ ,  $F_\beta$ , and  $\text{HL}_\beta$  were removed in the Ogasawara model because shrinkage exceeded 30%.

With regard to the covariate model, Stein et al. reported the full model as the final model for exploratory purposes. The %RSE of the estimated covariate effect were high (range 59–250%), which may indicate lack of information to support the effect estimation in the data. The covariates listed in Ogasawara et al., whereas estimated with reasonable %RSE (range 14–43%), simulation of the magnitude of covariate effects on the exposure metrics were smaller than the IIV in the population. Therefore, they were not considered to have a meaningful impact on liso-cel kinetics.

Although the current analyses did not allow identification of statistically significant effect among the covariates tested, this finding does not necessarily indicate a true lack of effect. Rather, it likely reflects either lack of information in the data (e.g., small sample size) to support the identification of true covariate effect, or lack of robustness of the usual covariate screening approach to identify the true covariate effect among large intersubject variability in the parameters. The intersubject variability can come from a mix of different sources, including subjects' demographics, baseline characteristics, and manufactured product characteristics, as well as heterogeneity in the CAR-T processes (trafficking, proliferation, memory cell formation, apoptosis, etc). Other emergent techniques, such as machine learning approaches, may be investigated to further identify the predictor covariates more precisely in the future.

## CONCLUSION

A population cellular kinetic model has been developed to adequately characterize CAR transgene level of ciltacel in blood following i.v. infusion of  $0.75 \times 10^6$  (range  $0.5\text{--}1.0 \times 10^6$ ) CAR-positive viable T-cells/kg body weight. Given the large intersubject variability at various aspects of ciltacel kinetics postinfusion, none of the investigated subjects' demographics and baseline characteristics and manufactured product characteristics showed statistically significant effect on CAR transgene levels. The developed

model also enables subsequent exposure-biomarker, exposure-efficacy, and exposure-safety analyses.

## AUTHOR CONTRIBUTIONS

L.S.W., Y.S., C.L., and H.Z. wrote the manuscript. L.S.W., Y.S., C.L., W.Z., C.C.J., Y.-N.S., and H.Z. designed the research. L.S.W., Y.S., C.L., W.Z., C.C.J., Y.-N.S., and H.Z. performed the research. L.S.W., Y.S., C.L., W.Z., Y.-N.S., and H.Z. analyzed the data.

## FUNDING INFORMATION

No funding was received for this work.

## CONFLICT OF INTEREST

L.S.W., Y.S., C.L., W.Z., and C.C.J. are current employees of Janssen R&D. Y.-N.S. and H.Z. are former employees of Janssen R&D.

## REFERENCES

1. Carpenter RO, Evbuomwan MO, Pittaluga S, et al. B-cell maturation antigen is a promising target for adoptive T-cell therapy of multiple myeloma. *Clin Cancer Res.* 2013;19(8):2048-2060.
2. Maus MV, June CH. Zoom zoom: racing CARs for multiple myeloma. *Clin Cancer Res.* 2013;19(8):1917-1919.
3. Avery DT, Kalled SL, Ellyard JI, et al. BAFF selectively enhances the survival of plasmablasts generated from human memory B cells. *J Clin Invest.* 2003;112(2):286-297.
4. De Boer RJ, Oprea M, Antia R, Murali-Krishna K, Ahmed R, Perelson AS. Recruitment times, proliferation, and apoptosis rates during the CD8(+) T-cell response to lymphocytic choriomeningitis virus. *J Virol.* 2001;75(22):10663-10669.
5. De Boer RJ, Perelson AS. Quantifying T lymphocyte turnover. *J Theor Biol.* 2013;327:45-87.
6. Chaudhury A, Zhu X, Chu L, et al. Chimeric antigen receptor T cell therapies: a review of cellular kinetic-pharmacodynamic modeling approaches. *J Clin Pharmacol.* 2020;60(Suppl 1):S147-S159.
7. Stein AM, Grupp SA, Levine JE, et al. Tisagenlecleucel model-based cellular kinetic analysis of chimeric antigen receptor-T cells. *CPT Pharmacometrics Syst Pharmacol.* 2019;8(5):285-295.
8. Ogasawara K, Dodds M, Mack T, Lymp J, Dell'Aringa J, Smith J. Population cellular kinetics of lisocabtagene maraleucel, an autologous CD19-directed chimeric antigen receptor T-cell product, in patients with relapsed/refractory large B-cell lymphoma. *Clin Pharmacokinet.* 2021;60(12):1621-1633.
9. Savic RM, Jonker DM, Kerbusch T, Karlsson MO. Implementation of a transit compartment model for describing drug absorption in pharmacokinetic studies. *J Pharmacokinet Pharmacodyn.* 2007;34(5):711-726.
10. Berdeja JG, Madduri D, Usmani SZ, et al. Ciltacabtagene autoleucel, a B-cell maturation antigen-directed chimeric antigen receptor T-cell therapy in patients with relapsed or refractory multiple myeloma (CARTITUDE-1): a phase 1b/2 open-label study. *Lancet.* 2021;398(10297):314-324.
11. Beal SL, Sheiner LB, Boeckmann AJ, Bauer RJ, eds. *NONMEM 7.4.3 Users Guides*. Icon Development Solutions; 1989–2019.

12. Ahn JE, Karlsson MO, Dunne A, Ludden TM. Likelihood based approaches to handling data below the quantification limit using NONMEM VI. *J Pharmacokinet Pharmacodyn.* 2008;35(4):401-421.
13. Beal SL. Ways to fit a PK model with some data below the quantification limit. *J Pharmacokinet Pharmacodyn.* 2001;28(5):481-504.
14. Bergstrand M, Karlsson MO. Handling data below the limit of quantification in mixed effect models. *AAPS J.* 2009;11(2):371-380.
15. Ette EI. Stability and performance of a population pharmacokinetic model. *J Clin Pharmacol.* 1997;37(6):486-495.
16. Savic RM, Karlsson MO. Importance of shrinkage in empirical bayes estimates for diagnostics: problems and solutions. *AAPS J.* 2009;11(3):558-569.

## SUPPORTING INFORMATION

Additional supporting information can be found online in the Supporting Information section at the end of this article.

**How to cite this article:** Wu LS, Su Y, Li C, et al. Population-based cellular kinetic characterization of ciltacabtagene autoleucel in subjects with relapsed or refractory multiple myeloma. *Clin Transl Sci.* 2022;15:3000-3011. doi: [10.1111/cts.13421](https://doi.org/10.1111/cts.13421)